DECISION-DIRECTED FINE SYNCHRONIZATION FOR CODED OFDM SYSTEMS

K. Shi , E. Serpedin, and P. Ciblat

Dept. of Electrical Engineering
Texas A&M University, College Station, TX 77843, USA.
Email: serpedin@ee.tamu.edu

ABSTRACT

A new decision-directed (DD) synchronization scheme is proposed for joint estimation of carrier frequency offset (CFO) and sampling clock frequency offset (SFO) in coded orthogonal frequency division multiplexing (OFDM) systems. By exploiting the decisions provided by a Viterbi decoder and the information available on all the modulated subcarriers, we report accurate estimators of residual CFO and small SFO without relying on pilots. The performance analysis and simulation results indicate that the proposed novel DD scheme achieves much better performance than the conventional pilot-based schemes in both AWGN and frequency-selective channels.

I. INTRODUCTION

Orthogonal frequency division multiplexing (OFDM) systems are well fit for high speed transmissions in highly frequency-selective (F-S) channels. However, OFDM is sensitive to synchronization errors. Numerous papers [1]-[3] deal with coarse frame (timing) and carrier frequency offset (CFO) synchronization while quite a few ones discuss the estimation of residual CFO and possible sampling clock frequency offset (SFO), the so called fine synchronization step. For coarse frame and CFO synchronization, most schemes [1]-[3] proposed estimators that operate before the fast Fourier transform (FFT) block present in the receiver. However, after coarse synchronization, there might still be present a residual CFO and uncompensated SFO, which will introduce large phase rotations even for short packets [4]-[5].

To remove the effect of CFO and SFO, some authors proposed pilot based post-FFT synchronizers [6]-[8]. Although the estimator [6] appears to work under general channel conditions, no analytical result has been reported to assess its unbiasedness in F-S channels. Also, the alternative estimator [8] appears to be biased in F-S channels. In this paper, we propose a new decision-directed (DD) post-FFT CFO and SFO synchronization scheme without using pilots. By utilizing the conjugate product of two consecutive OFDM symbols and the reliable decisions provided by a Viterbi decoder, we report first a one-shot DD joint estimation scheme of CFO and SFO. To obtain highly-accurate CFO and SFO estimates in F-S channels, the one-shot estimates are further passed through first-order tracking loop filters that are used to control the interpolator and frequency corrector blocks. It is shown that the proposed CFO and SFO estimators are unbiased and exhibit much better mean-square error (MSE) performance compared with conventional data aided schemes in both AWGN as well as F-S channels. Analytical closed-form expressions of the mean-square error (MSE) of proposed estimators are also reported for AWGN channels.

II. SIGNAL MODELS

In the transmitter of a coded OFDM system, the binary source data is passed through a convolutional encoder and block interleaver and Gray mapped into $a_{l,k}$, which denotes the complex data modulated on the $f_k = k/T_u$ subcarrier frequency of the l_{th} OFDM symbol, which is assumed of unit variance $E\{|a_{l,k}|^2\} = 1$. The transmitted complex baseband signal can be described by

$$s(t) = \frac{1}{\sqrt{T_u}} \sum_{l=0}^{\infty} \sum_{k=-K/2}^{K/2} a_{l,k} e^{j2\pi(k/T_u)(t-T_g-lT)} g(t-lT) \quad (1)$$

where $g(t)$ is a rectangular pulse with unit amplitude during $0 \leq t < T$. To avoid intersymbol interference (ISI) in frequency-selective channels, each symbol is preceded by a guard interval (cyclic prefix) of length T_g, which represents a repetition of the last portion of the symbol. To simplify the transmitter, we assume a discrete-time implementation (with the sampling period $T_s = T_u/N$) of $s(t)$, that can be easily generated by means of an N-point inverse fast Fourier transform (IFFT). In addition, K is chosen to be less than N to avoid spectrum aliasing. Therefore, the symbol period is $T = T_g + T_u$, which corresponds to $M = N + N_g$ samples.

If the transmitted signal is passed through the wide-sense stationary uncorrelated scattering (WSSUS) channel with channel transfer function (CTF)

$$h(\tau, t) = \sum_i h_i(t)\delta(\tau - \tau_i) \ , \quad (2)$$

the received signal sampled with the period T_s', in the presence of carrier frequency offset (CFO) f_e, timing offset $n_e T_s'$ and small sampling clock frequency offset (SFO) $\epsilon = (T_s' - T_s)/T_s$, is given by

$$r(nT_s') = e^{j2\pi f_e n T_s'} \sum_i h_i(nT_s') s(nT_s' - \tau_i - n_e T_s') + w(nT_s') \quad (3)$$

where each path $h_i(nT_s')$ presents a Rayleigh distributed amplitude and a uniformly distributed phase. The channel energy is assumed normalized to unity $\sum_i E[|h_i(nT_s')|^2] = 1$. To avoid ISI, the normalized maximum delay spread τ_{max} (normalized by T_s') is assumed less than the length of guard interval N_g. In addition, $w(nT_s')$ denotes complex additive white Gaussian noise (AWGN) with variance $\sigma_n^2 = E\{|w(nT_s')|^2\}$. The average signal-to-noise ratio (SNR) per symbol is defined as $E_s/N_o = 1/\sigma_n^2$.

After the coarse timing estimation step [1]-[2], $\hat{n}_e$ is used by the FFT window controller as shown in Fig. 1. Therefore, the FFT window can be assumed to start from the ISI-free area $[\tau_{max} +$

$1+lM, N_g+lM]T_s'$. There might be a small timing offset after coarse timing synchronization, which can be absorbed in CTF [5]. To reduce possible intercarrier interference (ICI), a coarse CFO estimate $\hat{f}_e$ is used by the frequency corrector block. The output of the N-point FFT block can be expressed as:

$$z_{l,k} = \frac{1}{\sqrt{N}} \sum_{n=0}^{N-1} r_{l,n} e^{-j2\pi kn/N} \ , \qquad (4)$$

where $r_{l,n} = r((n+N_g+lM)T_s')$. Taking into account the small SFO ϵ and residual CFO $f_N = f_e T_u$ (normalized by subcarrier spacing), after some manipulations similar to the ones in [5], the l_{th} symbol of the N-point FFT block takes the expression:

$$z_{l,k} \approx a_{l,k} H_{l,k} e^{j\pi\theta_k(N-1)/N} e^{j2\pi\theta_k(N_g+lM)/N} + n_{l,k} \ , \qquad (5)$$

where $n_{l,k}$ is AWGN noise with the same variance as w_n and

$$\theta_k = f_N(1+\epsilon) + \epsilon k \approx f_N + \epsilon k. \qquad (6)$$

In the approximate expression (5), the ICI caused by small CFO and SFO can be omitted since its power is very small with respect to the additive noise ($n_{l,k}$) power [4], [5]. We also omit the effect of slow drifts of the FFT window, caused by small SFO ϵ. However, the FFT window shift can be large enough to induce ISI if ϵ is not compensated. We also assume the channel to be constant during one OFDM symbol duration, and its taps are denoted by $h_{l,n} = h_n(lMT_s')$. Let $H_{l,k}$ denote the Fourier transform of the CTF

$$H_{l,k} = \sum_{n=0}^{\tau_{max}} h_{l,n} e^{-j2\pi k(n/N)} \ . \qquad (7)$$

In (5), the residual CFO and SFO introduce a time variant phase rotation $\phi_{l,k} = 2\pi\theta_k(N_g + lM + (N-1)/2)/N$, which depends on both the time index l and the subcarrier index k. Thus, for a certain value of l, the accumulated phase rotation $\phi_{l,k}$ can be large enough to introduce data decision errors. To avoid possible decision errors, we need to estimate and compensate $\phi_{l,k}$. Alternatively, we can estimate CFO f_N and SFO ϵ separately. For a feedback synchronization scheme, as we plan to utilize later, it is undesirable if the estimated parameter depends on the time index l. As suggested by [5], the effect of time index can be cancelled out by taking the conjugate product of two consecutive OFDM symbols

$$x_{l,k} = z_{l,k} \cdot z_{l-1,k}^* \approx e^{j2\pi\rho\theta_k} a_{l,k} a_{l-1,k}^* |H_{l,k}|^2 + \text{noise} \ , \qquad (8)$$

where $\rho = M/N$, $*$ denotes conjugate operation and the channel is assumed to be quasi-static $H_{l,k} \approx H_{l-1,k}$. To simplify subsequent discussions, we assume hereafter that $a_{l,k}$'s are M-PSK modulated data or pilots.

III. PREVIOUS RESULTS

A post-FFT data-aided (DA) CFO and SFO estimator was proposed in [6] and [7]

$$\hat{f}_N = \frac{1}{2\pi\rho} \frac{\varphi_{l,1} + \varphi_{l,2}}{2} \ , \quad \hat{\epsilon} = \frac{1}{2\pi\rho} \frac{\varphi_{l,2} - \varphi_{l,1}}{K/2} \ , \qquad (9)$$

where $\varphi_{l,(1|2)} = \arg\left[\sum_{k\in P_{(1|2)}} x_{l,k}\right]$, and $P_{(1|2)}$ takes the values 1 and 2 for the first and the second half of pilots, respectively. The pilots are assumed symmetrically and uniformly distributed around DC ($k=0$). It is easy to prove that estimators (9) are unbiased in the presence of AWGN and flat fading channels. In [7], the mean-square error of (9) in AWGN channels are reported:

$$\begin{aligned} \text{MSE}(\hat{f}_N) &= \frac{1}{4\pi^2\rho^2 N_P \cdot E_s/N_o} \ , \\ \text{MSE}(\hat{\epsilon}) &= \frac{4}{\pi^2\rho^2 K^2 N_P \cdot E_s/N_o} \ , \end{aligned} \qquad (10)$$

where N_P stands for the number of pilots per symbol. From (10), we can infer that the performance of estimators (9) can be improved by increasing the number of pilots N_P. However, increasing the number of pilots will decrease the system throughput.

IV. PROPOSED SYNCHRONIZATION SCHEME

IV-A. Decision-Directed Estimator

We notice that if data decisions $\hat{a}_{l,k}$ are available, they can be used to improve the performance of CFO and SFO estimators. For broadcasting systems, such as the European DVB system, reliable data decisions are available after the receiver has acquired some channel information based on the inserted pilots. Therefore, decision-directed (DD) schemes can be utilized to improve the tracking performance of CFO and SFO synchronizers in broadcasting systems. For burst transmission systems, such as the IEEE 802.11a standard, the synchronization preamble contains continuous pilots. Reliable data decisions $\hat{a}_{l,k}$ are available right after coarse synchronization and channel estimation. Thus, for burst OFDM transmission systems, we can use a DD scheme not only for tracking but also for acquisition. To make use of reliable decisions, the Viterbi decoder output is re-interleaved and re-mapped to the complex data decisions $\hat{a}_{l,k}$. Therefore, we propose the following estimator

$$\hat{f}_N = \frac{1}{2\pi\rho} \frac{\varphi_{l,1}' + \varphi_{l,2}'}{2} \quad , \quad \hat{\epsilon} = \frac{1}{2\pi\rho} \frac{\varphi_{l,2}' - \varphi_{l,1}'}{K/2+1} \qquad (11)$$

where

$$\varphi_{l,(1|2)}' = \arg\left[A_{l,(1|2)}\right], \ A_{l,(1|2)} = \sum_{k\in C_{(1|2)}} z_{l,k} \hat{a}_{l,k}^* z_{l-1,k}^* \hat{a}_{l-1,k} \qquad (12)$$

, and $C_1 = [-K/2, -1]$ and $C_2 = [1, K/2]$ denote the first and second half of data subcarriers, respectively. From (11), we expect that the performance of proposed estimators to be much better than performance of estimators (9) since all the data subcarriers have been utilized. In [9], we have shown that the MSEs of proposed estimators (11) in AWGN channels are given by

$$\begin{aligned} \text{MSE}(\hat{f}_N) &= \frac{1}{4\pi^2\rho^2 K \cdot E_s/N_o} \\ \text{MSE}(\hat{\epsilon}) &= \frac{4}{\pi^2\rho^2 K(K+2)^2 \cdot E_s/N_o} \ . \end{aligned} \qquad (13)$$

In [9], we have also shown that estimators (11) are unbiased in F-S channels for small ϵ. A similar proof can be carried out for the estimators (9) using some slight modifications.

From the simulation results presented in Fig. 2, we can observe that the one-shot estimation is not accurate enough for correction. One might expect that averaging over several symbols improves the performance. Unfortunately, in F-S channels, an error floor

is found for large SFO ϵ. As indicated in [9], the estimators (9) and (11) are not anymore unbiased in the presence of large SFO.

IV-B. Closed-Loop Synchronization Schemes

The above results suggest to utilize a closed-loop synchronization scheme in the presence of F-S channels. As long as the Viterbi decoder outputs reliable data decisions, the DD SFO and CFO estimators start to work. The one-shot estimates ($\hat{\epsilon}$ and $\hat{f_N}$) are post-processed by their corresponding first-order tracking loop filters

$$\hat{f}_l = \hat{f}_{l-1} + \gamma_f \hat{f_N}, \qquad \hat{\epsilon}_l = \hat{\epsilon}_{l-1} + \gamma_\epsilon \hat{\epsilon} \ . \tag{14}$$

Symbol by symbol, the above loop filters update the control parameters of number-controlled oscillators in the interpolator and frequency corrector. For large SFO, we first process coarse estimates. After correction with the first estimated value, a smaller residual SFO is left, and then a more accurate estimate is obtained. Finally, very accurate estimates can be expected in this feedback tracking scheme.

After convergence, the estimators exhibit small fluctuations about the stable equilibrium points. Considering a linearized equivalent model [10], we can derive the tracking performance of the closed-loop schemes as follows

$$\text{MSE} = \int_{-1/(2T)}^{1/(2T)} S(f)|H(f)|^2 df \ , \tag{15}$$

where $S(f)$ is the power spectral density (PSD) of loop noise present in CFO and SFO estimators (derived in [9])

$$\begin{aligned} S_{\text{CFO}}(f) &= \frac{\sigma_n^2[1-\cos(2\pi fT)]}{4\pi^2\rho^2 K} \\ S_{\text{SFO}}(f) &= \frac{4\sigma_n^2[1-\cos(2\pi fT)]}{\pi^2\rho^2 K(K+2)^2} \ , \end{aligned} \tag{16}$$

and $H(f)$ is the closed-loop transfer function given by

$$H(f) = \frac{-\gamma}{e^{j2\pi fT} - (1-\gamma)} \ . \tag{17}$$

From (16), we find that the loop noise is colored and its PSD is not flat across the loop bandwidth and presents a null at DC. Substituting (16)-(17) into (15), we can find the MSE of closed-loop DD estimators

$$\begin{aligned} \text{MSE}(\hat{f}_l) &= \frac{\gamma_f^2/(2-\gamma_f)}{4\pi^2\rho^2 K \cdot E_s/N_o} \\ \text{MSE}(\hat{\epsilon}_l) &= \frac{4\gamma_\epsilon^2/(2-\gamma_\epsilon)}{\pi^2\rho^2 K(K+2)^2 \cdot E_s/N_o} \ . \end{aligned} \tag{18}$$

Similarly, we obtain the MSE of closed-loop DA estimators in [6] and [7]

$$\begin{aligned} \text{MSE}(\hat{f}_l) &= \frac{\gamma_f^2/(2-\gamma_f)}{4\pi^2\rho^2 N_P \cdot E_s/N_o} \\ \text{MSE}(\hat{\epsilon}_l) &= \frac{4\gamma_\epsilon^2/(2-\gamma_\epsilon)}{\pi^2\rho^2 K^2 N_P \cdot E_s/N_o} \ , \end{aligned} \tag{19}$$

which suggests that the previous result in [7], which assumes a flat PSD of loop noise within the loop bandwidth, is too pessimistic.

V. COMPUTER SIMULATIONS

In our simulations, we assume an OFDM system with $N = 128$ subcarriers and guard interval of 16. There are 10 pilot subcarriers inserted into 120 QPSK data modulated subcarriers in the DA scheme, while no pilot is inserted in the DD scheme. We assume a 12-path frequency-selective channel with exponentially decaying power profile and the root-mean square (RMS) delay spread is $1.25\ T_s$. We assume the channel is static during the whole packet (150 symbols).

Further, we utilize a rate $1/2$ convolutional encoder with generator polynomial (133,171) and a block (16x15) interleaver to combat additive noise and spectral nulls, respectively. The simulation results are obtained using 2,000 Monte-Carlo trials for each SNR value. The SFO ϵ and CFO f_N are assumed equal to 40 ppm and 0.06, respectively.

In Fig. 2, we show the one-shot estimation performance for DD and DA estimators. Simulation results show a good agreement between the analytical (analysis) results and the experimental results. Also, the proposed DD estimator is about 10 dB better than the DA scheme in both AWGN channels as well as F-S channels.

Next, we resort to the closed-loop scheme as described in Section IV-B, and consider $\gamma_\epsilon = 0.069$ and $\gamma_f = 0.081$ for both DD and DA schemes. As shown in Fig. 3, the one-shot estimates are smoothed by loop filters and the residual errors in the proposed DD scheme converge to zero within 30 symbols. The closed-loop tracking performance of DD scheme in Fig.4, which is much better than that of the conventional DA scheme for both CFO and SFO synchronization, corroborates the closed-loop analysis results presented in Section IV.

VI. CONCLUSIONS

We have introduced a new decision-directed post-FFT joint estimator for carrier frequency offset and sampling clock frequency offset in coded OFDM systems. By performance analysis and computer simulations, we have shown that the proposed new scheme exhibits much better performance compared to conventional data-aided scheme in both AWGN and frequency-selective channels. Since we save the pilots for synchronization, the throughput of system is increased. With very few additional hardware, this new synchronization scheme can be implemented in many wireless OFDM systems.

VII. REFERENCES

[1] T. M. Schmidl, and D. C. Cox, "Robust frequency and timing synchronization for OFDM," *IEEE Trans. on Commun.*, Dec.1997.

[2] J. J. van de Beek, M. Sandell, and P. O. Borjesson, "ML estimation of time and frequency offset in OFDM systems," *IEEE Trans on Signal Processing*, July 1997.

[3] K. Shi, and E. Serpedin, "Coarse frame and carrier synchronization for OFDM systems: a new metric and performance evaluation," *IEEE Trans. on Wireless Commun.*, accepted, Aug. 2002.

[4] T. Pollet, et. al., "The BER performance of OFDM systems using non-synchronized sampling," *Proc. GLOBECOM*, 1994.

[5] M. Speth, S. A. Fechtel, G. Fock, and H. Meyr, "Optimum Receiver Design for Wireless Broad-Band Systems Using OFDM–Part I," *IEEE Trans. on Commun.*, Nov. 1999.

[6] M. Speth, S. A. Fechtel, G. Fock, and H. Meyr, "Optimum Receiver Design for Wireless Broad-Band Systems Using OFDM–Part II," *IEEE Trans. on Commun.*, April 2001.

[7] S. A. Fechtel, "OFDM carrier and sampling frequency synchronization and its performance on stationary and mobile channels", *IEEE Trans. on Cons. Elec.*, Aug. 2000.

[8] B. Yang, K. B. Letaief, R. S. Cheng and Z. Cao, "Timing recovery for OFDM transmission," *IEEE Journal on Selected Areas in Commun.*, Nov. 2000.

[9] K. Shi and E. Serpedin, "Decision-Directed Fine Synchronization for Coded OFDM systems," *submitted to IEEE Trans. on Comm.*, Sept. 2003.

[10] H. Meyr, et. al., *Digital Communication Receivers: Synchronization, Channel Estimation and Signal Processing*, John Wiley & Sons Inc., 1998.

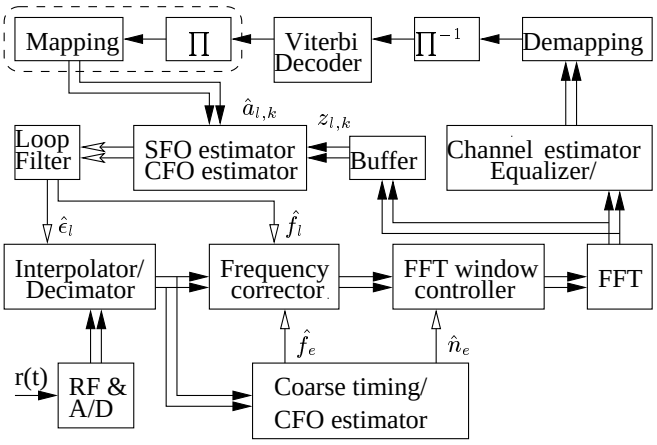

Fig. 1. The receiver structure of coded OFDM systems.

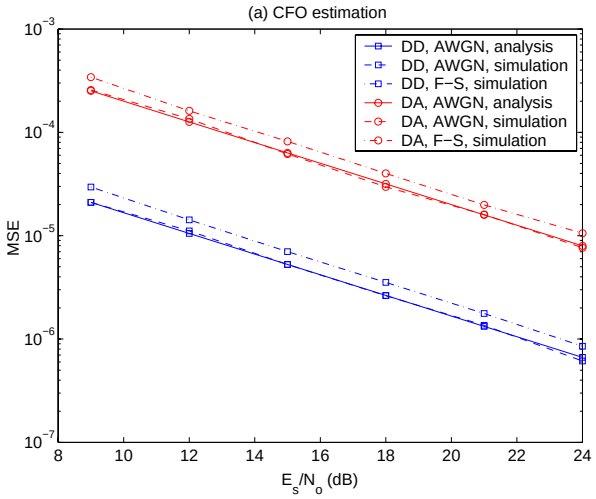

Fig. 2. The one-shot estimation performance.

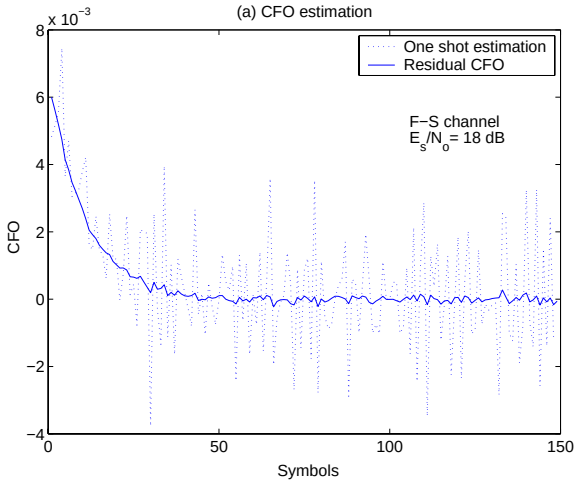

Fig. 3. Convergence of DD closed-loop synchronization

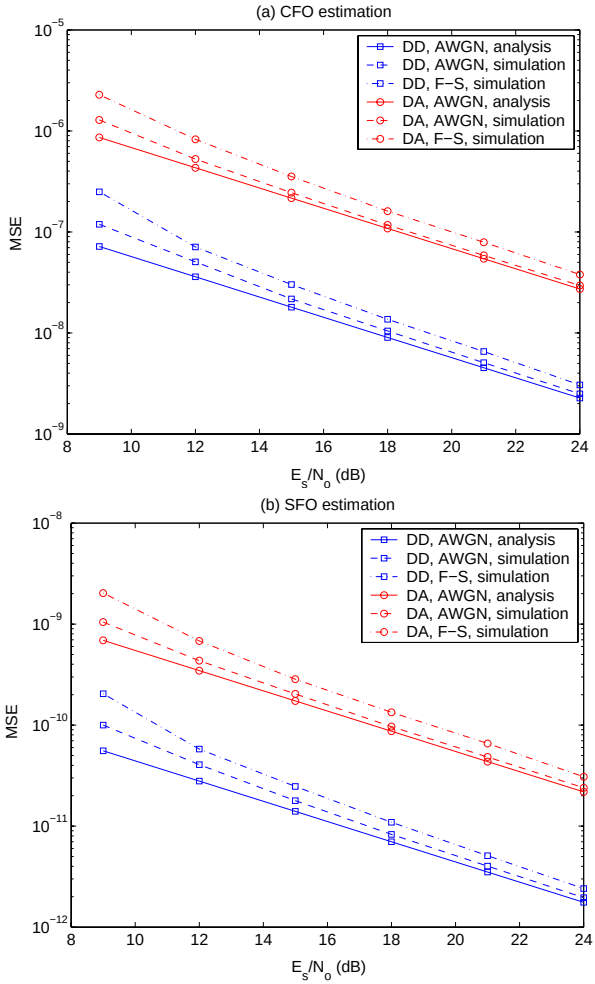

Fig. 4. The closed-loop performance